Physically-Based Modelling of Double-Peak Discharge Responses at Slapton Wood Catchment

Stephen J Birkinshaw

School of Civil Engineering and Geosciences

University of Newcastle upon Tyne

Newcastle upon Tyne

NE1 7RU

s.j.birkinshaw@ncl.ac.uk

Tel. 0191 2228836

Abstract

Heavy winter rainfall produces double-peak hydrographs at the Slapton Wood catchment, Devon, UK. The first peak is saturation-excess overland flow in the hillslope hollows, and the second (i.e. the delayed peak) is subsurface stormflow. The physically-based spatially-distributed model SHETRAN is used to try and improve the understanding of the processes that cause the double peaks. A three-stage (multi-scale) approach to calibration is used: (1) water balance validation for vertical one-dimensional flow at arable, grassland and woodland plots; (2) two-dimensional flow for cross-sections cutting across the stream valley; and (3) three-dimensional flow in the full catchment. The main data are for rainfall, stream discharge, evaporation, soil water potential, and phreatic surface level. At each scale there was successful comparison with

measured responses, using as far as possible parameter values from measurements. There was some calibration but all calibrated values at one scale were used at a larger scale.

A large proportion of the subsurface runoff enters the stream from three dry valleys (hillslope hollows), and previous studies have suggested convergence of the water in the three large hollows as being the major mechanism for the production of the delayed peaks. The SHETRAN modelling suggests that the hillslopes that drain directly into the stream are also involved in producing the delayed discharges. The model shows how in the summer most of the catchment is hydraulically disconnected from the stream. In the autumn the catchment eventually 'wets up' and shallow subsurface flows are produced, with water deflected laterally along the soil-bedrock interface producing the delayed peak in the stream hydrograph.

Key Words

double-peak hydrograph; physically-based distributed model; Slapton Wood; SHETRAN; catchment modelling; saturation excess overland flow; subsurface stormflow

Introduction

At the Slapton Wood catchment (Figures 1 and 2), there are double peaks in some of the storm hydrographs (Burt and Butcher, 1985a). A typical double peak is shown on the right hand side in Figure 3. Burt and Butcher (1985b) suggested that the first peak is saturation-excess surface runoff, and the second, which occurs up to several days after

rainfall, is shallow subsurface runoff. The second peak is rounded in nature with a gradual increase in stream discharge followed by a gradual recession. It is thought that infiltrating water produces a perched layer, and water is deflected laterally, flowing down slope to the stream (Weyman, 1973). There are double peaks only when the catchment is wet. When it is dry, there are low flows and short-lived single peaks. The low flows are thought to be sustained by groundwater flowing at depth through fractures in extensively folded slates (Burt and Heathwaite, 1996; Chappell and Franks, 1996).

Similar double peaks have been seen in other catchments (Anderson and Burt, 1978; Chevallier and Planchon, 1993; Hihara and Susuki, 1988; Weyman, 1973). Other causes for delayed peaks in double-peak responses include subsurface flow in the hydromorphic zone that surrounds a valley bottom (Masiyandima et al., 2003), tunnel-type bedrock flow in areas underlain by limestone (Hirose et al., 1994; Lakey and Krothe, 1996), and subsurface flow through fractured bedrocks in sedimentary rocks (Agata and Tanaka, 1997; Onda et al., 2001).

There appears to have been very little modelling work carried out at other catchment where delayed peaks from shallow subsurface runoff are important. However, there have been a significant number of attempts to model the Slapton Wood catchment and these have produced mixed results. A simple model was used by Burt and Butcher (1985a) to study delayed peaks. This was based on data and descriptions from Slapton Wood, but involved simulations of hypothetical hillslopes. They studied the role of rainfall and antecedent soil moisture in controlling the size and timing of delayed peaks and drew the conclusion that soil-water convergence in the hillslope hollows plays a major role. Fisher (1995) used the distribution function model TOPMODEL. He found it necessary to use two sets of parameters, arguing that there are two ‘stores’, with

different time constants. The first ‘store’ represents perched water, and the second ‘store’ the saturated fractured bedrock. TOPMODEL was also used by Fisher and Beven (1996), but this time within the GLUE uncertainty-handling methodology (Beven and Binley, 1992), as did Beven and Freer (2001), but using a dynamic version of TOPMODEL. The dynamic version allows the simulation of a dynamically variable upslope contributing area and produced slightly better results. None of the TOPMODEL studies was designed to examine the processes that result in double peaks. There have been previous SHETRAN simulations of Slapton Wood, including Bathurst et al. (2004) who carried out a ‘blind’ validation (Ewen and Parkin, 1996). This tested the ability to predict the discharge at the outlet of the catchment, plus some internal responses such as phreatic surface depths, without the use of calibration (hence the calibration was ‘blind’). Although this validation was considered successful, double peaks were not simulated because Version 3 of SHETRAN was used and it is unable to simulate shallow subsurface flow. In Version 4, the subsurface is modelled as a fully three-dimensional variably saturated medium (Ewen et al., 2000), but although this allows shallow subsurface flow to be simulated, the simulation of double peaks was poor (Birkinshaw and Ewen, 2000).

The aim of the work in this paper is to try and explain the physical processes that occur within Slapton Wood and how the double peaks are produced. To do this a physically-based spatially-distributed model is necessary as these models directly represent the physically processes. A large number of physically-based spatially-distributed models have been developed [e.g. MIKE SHE (Graham and Butts, 2006), SWAT (Arnold et al., 1998), WATFLOOD (Bingeman et al., 2006)] and a review of the mathematical basis of eleven of these models can be found in Borah and Bera (2003).

Previous studies in Slapton Wood have shown the importance of shallow subsurface flow and most of the physically-based spatially-distributed models do not incorporate the three-dimensional variably saturated equations (Panday et al., 1993) necessary to simulate this flow. Two suitable models are MODHMS (Panday and Huyakorn, 2004) and SHETRAN Version 5 (Ewen, 2001). SHETRAN Version 5 was selected for this work as it has an accurate and robust solver for subsurface flow, plus strong surface-subsurface coupling based on the approach described by Zhang and Ewen (2000).

Recently, Ewen and Birkinshaw (2006) used a "downward" approach (sometimes called a "data-based" or "top-down" approach) to develop a lumped hysteretic model that can reproduce the double-peak responses. This model is based directly on the rainfall and discharge data, and during its development no assumptions were made about the physical process that take place within the catchment. It was argued by Ewen and Birkinshaw (2006) that the best way to develop reliable models is to combine "downward" and "upward" steps. SHETRAN is a classic example of an "upward" model, because, it uses "bottom up" modelling based on applying physical laws on a fine grid. A physical interpretation for the delayed peak was developed in Ewen and Birkinshaw (2006), but it was noted that more than one interpretation is consistent with the lumped hysteretic model.

Catchment and Monitoring

The Slapton Wood catchment covers 0.94 km^2, 60% of which lies above the 90m contour. Above 90m, the slopes are gentle, generally less than 5%, and the land is intensively farmed, mainly as grassland and for cereal and root crops. Below 90m, the

slopes are steeper, up to 25%, and there is permanent grassland and a wood (which covers 13.5% of the catchment). The soils are mainly freely-draining acid brown soils with a clay-loam texture (Trudgill, 1983). Solifluction head deposits have been found below the soils (Chappell and Franks, 1996), mainly on the western side of the catchment, and were observed to produce a saturated layer, above the unsaturated slate below. Percolation is impeded because of the fine matrix and the presence of local 'fragipan' layers. The head deposits are underlain by extensively folded slates (Chappell and Franks, 1996) with a dip of 70° to the south. Figure 1 shows that the stream is fed by three large hillslope hollows on the western side (namely, Loworthy, Carness and Eastergrounds hollows, in order north to south).

The Slapton research catchments (of which Slapton Wood is one) have been monitored over a long period [see Burt and Horton (2001) for climatology and Burt and Heathwaite (1996) for hydrology]. The main data used here are for short-term intensive monitoring in 1989-1991. Precipitation, net radiation, wind speed, air temperature and vapour pressure deficit are available from an automatic weather station for the grassland plot (Figure 1) from 16th November 1989 to 31st March 1991. Three ground-level storage gauges were read manually on a weekly basis and the data used to calculate the spatial variation of precipitation. Discharge was measured at the catchment outlet, using a V-notch weir installed in 1971, every 15 minutes from 13th September 1989 to 31st March 1991. Soil water potential was measured using mercury manometer tensiometers at the arable, grassland and woodland plots, at three locations in each plot, from 6th September 1989 to 31st March 1991, approximately twice a week at depths from 0.2m to 1.2m. In September 1990, to record potentials for dry conditions, two sets of gypsum blocks were installed at the grassland plot. Thirty two dipwells (15 installed in

September 1989, two in June 1990 and 15 in September 1990), were dipped approximately every week from September 1989 to March 1991. The drilled depth varied from well to well, from 0.88m to 25m, depending on location.

SHETRAN and Calibration

SHETRAN Version 5 (Ewen, 2001) is a finite-difference model for water flow and heat and solute transport in river catchments in which the physics-based governing partial differential equations for flow and transport are solved on a three-dimensional grid. It is usually described as a physically-based spatially-distributed modelling system, to distinguish it from, simpler, and less-flexible, conceptual and lumped models. The advantage of using a physically-based spatially-distributed model in this work is that it gives a direct, three-dimensional, representation of the catchment and direct representations of physical processes.

The grid used for Slapton Wood has a 50 m square mesh when viewed in plan (Figure 1). The columns associated with mesh squares are called sub-units (Figure 2). These are divided into many cells, by horizontal slicing. Physical properties can vary from sub-unit to sub-unit and cell to cell, and the state of the catchment at any time is simply represented by the states (e.g. head, moisture content and temperature) of the cells. An important aspect of this work is that the calibration of SHETRAN for Slapton Wood was carried out in three stages. Stage 1 was for vertical one-dimensional (1-D) flow in columns, at each of the representative plots (arable, grassland and woodland); stage 2, for two-dimensional (2-D) water flow at two cross-sections that cut across the catchment (shown in Figures 1 and 2); and stage 3, for three-dimensional (3-D) flow in the full catchment. The aim in each stage was to produce a good match between the

field measurements and simulated variables, while using measured or literature parameter values wherever possible. Once a stage was complete, the calibrated parameter values were used in the next stage. The idea behind this staged (or multi-scale) approach is that it avoids some of the parameter compensation problems that can arise in calibration (e.g. see (Ewen et al., 2006), which also uses the data from Slapton Wood). It seems reasonable, for example, that the parameters for 1-D vertical flow are calibrated using point-scale observations, rather than being calibrated as part of a general calibration of the 3-D model against the outlet hydrograph.

1-D Simulations

The aim in calibration was to achieve simulations that are self-consistent, and which give evaporation similar to that estimated by the Institute of Hydrology (1993) and soil potentials similar to the those observed. The relevant calibrated parameters for the 1-D simulations are shown in Table I for the three plots. A comparison of calculated and simulated evaporation is shown in Table II, and potentials in Figure 4. This calibration was considered successful. There are problems accurately measuring soil water potential, so a close match cannot be expected in Figure 4. Also, there was considerable spatial variation over small distances when making measurements in the field, but the simulation has a single value for a 50 m square. Following the technique used in Bathurst et al. (2004), therefore, Figure 4 shows the observed potential at one measurement location in each plot.

The simulations are all for a 2m deep sub-unit with 15 cells varying in thickness from 0.02m at the ground surface to 0.2m at the base. The soil parameter values for the clay loam were as used in previous studies (Bathurst et al., 2004; Birkinshaw and Ewen,

2000), and are based on measurements. The parameters are: saturated moisture content 0.4; residual moisture content 0.12; saturated hydraulic conductivity 0.5 m/day; van Genuchten α parameter 1.0 m^{-1}; and van Genuchten n parameter 1.6.

The uncalibrated vegetation parameter values are from the previous studies, and literature values (Breuer et al., 2003), but the leaf area indeces for grassland are lower than typically found (Breuer et al., 2003), because the grassland is intensively grazed. The arable simulation used a time-varying root density function, which follows the same annual variation as the leaf area fraction, with the roots reaching a maximum depth of 0.5m just before harvest. Transpiration was assumed affected by the soil water potential (factor calibrated).

In the field containing the arable plot, barley was grown in the winter of 1989/1990, and the field planted to grass in July 1990. In the simulation, 11.1% of the evaporation was intercepted precipitation, which is very similar to the estimated value (12.8%). The arable simulation correctly shows the soil as nearly saturated at both 0.2m and 1.2m during both winters, and correctly shows it drying in spring 1990, drying faster at 0.2m. By the end of April 1990, the simulated soil water potential drops below –10m, when there are no observations because the soil became too dry for the tensionmeters. At 1.2m, the simulated potential is below that observed during the spring and early summer 1990, but the trends are similar. In autumn 1990, there are few observations, but the simulation correctly shows the soil wetting up. By November 1990 both the simulated and observed values show that the soil is nearly saturated.

Grass has been grown for several years in the field containing the grassland plot, and was grazed by cows and sheep. Figure 4 shows good agreement between the simulated and observed potentials at both 0.2m and 1.2m. In particular, the timings of

the drying in the spring and wetting up in the autumn are accurate. However, the simulated potentials in autumn 1990 are not as low (i.e., dry) as observed using the using the gypsum blocks (installed in autumn 1990).

The woodland plot is a mature deciduous woodland. In total, 38.8% of the simulated evaporation was from the canopy, which is very similar to the estimated value (36%). The simulation shows high evapotranspiration in May and June 1990, and that there is drying over the whole 2m deep profile, because the roots are deeper than for the other plots. At 0.2m depth during this period, therefore, it is wetter in the woodland plot than in the other plots. However, the high evapotranspiration during the rest of the summer causes the entire profile at the woodland site to dry, so that by the middle of August 1990 the woodland plot is the driest, at both 0.2m and 1.2m. The drying continues until autumn, and the woodland site is the last to completely wet up in December 1990.

Table II shows that the woodland plot has the largest annual evaporation followed by the grassland and the arable plots. The main differences are associated with high evaporation of intercepted rainfall from the woodland canopy, as a result of the large leaf area fraction of the deciduous trees in the summer, and low transpiration at the arable plot after harvest.

2-D Simulations

Two cross-sections were selected to run the simulations and the position of these can be seen in Figure 1. The aim in calibration was to run 2-D simulations that give discharges to the stream consistent with the observed catchment outlet discharge. Some conclusions will be drawn from the results of these simulations, as to the nature of the processes creating second (delayed) peaks. The relevant calibrated parameters for the

2-D simulations are shown in Table III. These are the hydraulic properties that control the creation and drainage of perched water bodies.

Cross-section 1 (Figure 2) is typical of cross-sections in the central and northern part of the catchment and shows a convex shape on the western side of the cross-section with a gently sloping plateau area and then a steep slope down to the stream. Cross-section 2 is steeper and does not have the plateau area, it is typical of the cross-sections in the southern part of the catchment. Land use is shown in Figure 2. The arable land is farmed with a rotation including winter barley, potatoes and temporary grassland. In the 2-D simulations, the arable vegetation is winter barley.

The sub-units are also shown in Figure 2. Most of these derive directly from the 50 m mesh, but a special mesh-nesting capability within SHETRAN Version 5 has been used so that 5 m wide sub-units can be used for the stream (these are sub-units 14 in cross-section 1 and 12 in cross-section 2, represented simply as lines in Figure 2.

A no-flow boundary condition was specified at the base and sides of the modelled area. Very little is known about the spatial variation in the thickness of the soil and depth to the bedrock, and each sub-unit was specified as being 20m deep containing four different media layers. The topsoil is 1.5m of clay loam. Below this, from 1.5m to 2.2m, there is a clay loam, which allows rapid subsurface lateral flows to the stream. (macropore flow has been observed in the catchment (Coles and Trudgill, 1985)). This layer corresponds to the head deposits described by Chappell and Franks (1996), who comment that there is a complete dearth of information about the conductivity of the deposits, and the properties of this layer were calibrated to allow rapid flow. On the steep valley sides and the eastern side of the catchment, the soils are generally shallower than this (Burt and Butcher, 1985b; Chappell and Franks, 1996), but allowing for such

variation was considered to add too much complexity to the modelling at this stage. From 2.2m to 2.7m below ground there is a low-conductivity slate layer, which is consistent with the observations of Chappell and Franks (1996) that there can be perching above this layer and artesian discharge as a result of augering through the layer. From the base of the low-conductivity layer to the 20 m there is fractured slate. The stream sub-units are exactly the same as the other sub-units, except that the topmost 2.2 m has a higher-conductivity layer, to make it more consistent with observations of alluvium deposits below the stream (Trudgill, 1983),

The properties of clay loam 1 (Table III) are exactly as in the 1-D simulations. For clay loam 2, the van Genuchten parameters and the saturated hydraulic conductivity were calibrated to give rapid flow, but special attention was paid to the flows simulated in saturated and near-saturated conditions, and the need to be reasonably consistent with the high saturated conductivities measured for this layer by Burt and Butcher (1985b) and Burt and Arkell (1986) (up to 86 m/day). For slate 1 and slate 2, the van Genuchten parameters and the saturated and residual moisture contents are as used by Birkinshaw and Ewen (2000), but their saturated hydraulic conductivities were calibrated. The saturated hydraulic conductivity for the clay loam under the stream channel was also calibrated.

The simulated discharge for the two cross-sections is shown in Figure 3. Cross-section 1 is typical of the majority of the catchment, so the fact that the results for cross-section 2 are worse than for cross-section 1 is acceptable It is encouraging that the results are good throughout the year, and not just during double-peaked events in the winter. In summer, the simulated discharge is correctly sustained by deep groundwater flows through the slate, and fairly constant low flows and short-lived single–peaks. In

winter, subsurface flow is important, and again this is captured well by the simulations. The observations show that the largest precipitation event, 3rd February 1990, produces an immediate peak, followed 24 hours later by a second peak As expected the first peak is not simulated, as it thought to occur due to saturation excess flow in the catchment hollows, but the delayed peak is well reproduced for both cross-sections, resulting from simulated lateral subsurface flow in the perched layer lying on the low–conductivity layer. What little surface flow and immediate peaks are simulated, are the result of precipitation on the stream.

Figure 5 shows the vertical flow in sub-unit 4 for cross-section 1 at different depths below ground. Throughout the year, at 10cm depth there is always vertical flow following precipitation. At 50cm, there is also always vertical flow, but in the summer it is considerably reduced compared with the 10cm depth. At 2m depth, though, there is no vertical flow in the summer, as all the precipitation has replaced previously evaporated water further up the profile. It is only at the end of November 1990 that the soil above 2 m has been sufficiently wetted for the vertical flow at 2 m to be re-established. This helps explain the difference between summer and winter runoff, because lateral subsurface flow occurs only when there is perching at the upper boundary of the low-conductivity slate layer (i.e. at 2.2 m depth), and this perching can become established only after November

The subsurface flow along cross-section 1 for the 3rd February 1990 event can be seen in Figure 6. Prior to the rainfall, the plateau area is fully hydraulically connected to the stream. The discharge from each sub-unit therefore increases as the stream is approached (i.e. it increases from sub-unit 1, on the plateau, to sub-unit 14) It can be seen in Figure 6 that, prior to rainfall, there is perching along most of the cross-section,

with the saturated thickness being greatest near and under the stream Following the precipitation, the flow from each sub-unit starts to increase after several hours, and it reaches a maximum after 24 hours. Note, that saturation is not reached on the steep slope at sub-unit 12, but it comes very close to saturation.

A different double-peaked event from 22nd February 1991 is shown in Figure 7, for which the prior conditions are quite different to those for 3rd February 1990. Prior to the rainfall, the plateau on the western side of the cross-section is hydraulically disconnected from the stream. There is some flow from the plateau to the stream, but it is flow through the fractured slate. The eastern side is hydraulically connected to the stream, so has a response similar to that for the 1990 event. The flow diagram in Figure 7 shows that a wetting front develops as perching is gradually established along the western plateau (sub-units 4-10), and it takes some 48 hours after rainfall before the plateau is fully hydraulically connected to the stream and the discharge rate into the stream reaches its maximum (compared to the 24 hours to reach the maximum in the 1990 event). The peak flow, 0.002 m^3/s, is much smaller than for the 1990 event, 0.012 m^3/s.

Although the 1990 event was larger (38mm compared to 20mm) much of the difference in response can be attributed to the antecedent conditions. The 1991 event had dry antecedent conditions (48mm in the previous 20 days) and the plateau was initially hydraulically disconnected from the stream, whereas the 1990 event had wet antecedent conditions (178mm in the previous 20 days) and the plateau was already fully hydraulically connected to the stream.

It therefore appears that once the plateau becomes hydraulically connected to the stream, there is a step change in the subsurface discharge rate to the stream, because the

entire hillslope can then contributes to the delayed peak. This is entirely consistent with existing results from analysing the observed catchment discharge hydrograph. Butcher (1985) found two distinct delayed responses: (A) larger responses, for which he concluded a 'saturated wedge' had already developed and in which there was a relatively quick delayed response; and (B) smaller responses, for which the 'saturated wedge' developed only after the rainfall, so had a slower delayed response and lower peak discharge. Ewen and Birkinshaw (2006) showed their lumped hysteretic model, based solely on analysing the observed rainfall and discharge, is equivalent to a conventional-looking two-bucket cascade lumped model. One bucket, which can be thought of as representing the plateau, discharges into the other bucket, which can be thought of as representing the riparian zone, from where there is discharge to the stream. However, the two buckets are not linked in a conventional fashion, because the rate of discharge from the plateau bucket depends on the storages in both buckets. This, they argue, reflects the fact that the plateau cannot drain to the stream until both the plateau and riparian zones are quite wet (i.e. for there to be a strong hydraulic link between the plateau and the stream, the saturated areas in the riparian and plateau zones must meet and be well connected). They also noted, however, that other physical interpretations are possible.

3-D Simulations

The 3-D simulations used the parameters calibrated in the previous two stages, except for the surface flow properties, which are calibrated in this stage. The calibration is against the observed catchment outlet hydrographs. A no-flow boundary condition was defined around the edges and base of the modelled catchment, and the time period simulated was 16th November 1989 to 31st March 1991.

Figure 8 shows the full hydrograph and a detailed plot of the response for 3rd February 1990. Unlike for the 2-D cross-section simulations, there is a significant response associated with surface flow. Overall, there is a good correspondence between the simulated and measured discharge, but the simulated low flows are a little high in the summer. The low flows are sustained by groundwater flow in the fractured slate layer, and there is scope for improving the calibration for this layer. At the end of December 1990, there is a sudden change in the hydrological response with subsurface flow becoming important. The timing of this is accurate in the simulation. The double peaks are reasonably well simulated, although the simulated discharge is too low in the major event on 3rd February 1990. There is again scope for improvement here. For example, infiltration-excess overland flow from the roads and paths is not represented in the model.

The cause of the first peak can be seen in Figure 9, which shows the surface water depth on 3rd February 1990. The phreatic surface level has risen to the surface in two of the (usually) dry valleys, resulting in surface saturation and saturation-excess overland flow.

Many of the dipwell measurements are thought not to be reliable, as many of the readings correspond to the bottom of the wells. In Figure 10, the reliable data for 10th October 1990 are compared against the simulated phreatic surface depth. The phreatic surface is correctly shown as being close to the ground surface near the stream channel and in the hollows, deeper on the flatter areas on the western side of the catchment, and deepest on the steepest slopes.

Looking at time series of dipwell measurements only two sites (14,18 and 14,20) cover the entire period of the simulation from November 1989 to March 1991. The

comparison between measured and simulated phreatic surface levels for site (14,18) is shown in Figure 11a and the position of the site in Figure 10 (the response at site (14,20) is similar). There are significant differences between the measured and simulated values but they rise and fall at similar times of the year in response to precipitation events and they both remain fairly constant at a similar depth during the summer. However, the simulated phreatic surface depth rises to zero during the winter of 1989/1990, whereas, the measurements rise to only 0.7m below ground. There are problems comparing the simulated phreatic surface level, which is the average of a 50m x 50m grid square and the measured value, which is a point measurement. This 'scale problem' is a well known criticism of physically-based spatially-distributed models (Blöschl and Sivapalan, 1995) and although the grid size is only 50m x 50m, in this particularly case the scale problem is important as the grid square is near the stream channel where there a large changes in response over short distances. Differences between the simulated and measured stream water levels will also affect flow from the grid square and so are another source of error in the simulated phreatic surface level. This version of SHETRAN allows sub-grid refinement and future simulations should include more details near stream channels.

The comparison between measured and simulated phreatic surface level for site (10,14) is shown in Figure 11b and the position of the site in Figure 10. This site is located a long way from the stream, so has a different response compared to that in Figure 11a. Data are available only from September 1990 to March 1991. There are three dipwells at the site, and the simulated phreatic surface depths agrees quite well with the observations from dipwell 3. The wells are in extensively folded slate, where

the layer slope can be 70°, and this, perhaps, explains the large variation seen between these three quite closely drilled wells.

Discussion and Conclusions

A staged (multi-scale) approach has been used to calibrate the latest version (Version 5) of the physically-based spatially-distributed model SHETRAN, to reproduce the double-peaked responses observed during wet periods in the winter at the 0.94 km^2 Slapton Wood research catchment. This involved first calibrating the vegetation parameters (at the point-scale) to obtain good mass balances, then calibrating the hydraulic properties for lateral flow, for cross-sections intersecting the channel, then calibrating the surface flow properties in simulations of the whole catchment. The calibration simulations therefore progressed from 1-D columns, to 2-D cross-sections, to the 3-D whole catchment.

The aim throughout was to achieve the best physical representation of the processes that are thought to occur, in the expectation that this will help improve the understanding of the pathways by which water flows to the stream. Double-peak responses were reasonably well simulated, as were single peak responses in the summer. Internal observations were reasonably well reproduced, including soil water potential, phreatic surface level and evaporation rates.

The SHETRAN simulation shows how in the summer the soils on the plateau area are hydraulically disconnected from the stream channel. Any precipitation on the plateau is either stored in the soil or evaporated. In the late autumn, water infiltrates to 2m below ground at the top of the slate layer, where it is deflected laterally along the soil-slate interface. However, the soils on the plateau area remain disconnected from the

stream as the drier, steeper stream sides prevent lateral flow. Eventually these areas 'wet-up' and significant lateral subsurface flows occur, which produces the second peak in the hydrographs following precipitation events. A similar mechanism for the production of the delayed peak hydrograph was suggested from field measurements (Burt and Butcher, 1985a) and using a "downward" modelling approach (Ewen and Birkinshaw, 2006). It is encouraging that the SHETRAN model is able to reproduce the delayed peak hydrograph and the water flow pathways suggested by the model are similar to those found using measurements and a "downward" approach. However, this does not confirm that the model is correct in representing the fine details of the physical processes that produce the delayed peaks. It is suggested that detailed SHETRAN modelling is carried out for the Eastergrounds hollow using the existing measurements (Butcher, 1985) on the small-scale pattern of saturation within the hollow and discharge from the Eastergrounds spring.

There appears to be a lack of consensus in the literature concerning the role of the spurs and hollows in the development of the delayed hydrograph. Flow through the three hollows (Loworthy, Carness and Eastergrounds) accounts for about 60% of the catchment area and Burt and Butcher (1985a,1985b) emphasised the convergence of the water in these three large hillslope hollows as being a major mechanism in the production of the delayed peaks. However, Burt and Arkell (1986) carried out dilution gauging along the river and found the steep valley side and spurs account for consistently higher unit area runoff than the hollows. Although, these measurements included winter periods they were unable to carry out measurements during a delayed event. They suggest that these areas are also important during delayed peaks but the hollows may become relatively more important. This work has shown that the delayed

peak hydrograph can be produced on the hillslopes that directly feed the stream as well in the hollows where there is the convergence of water. Further work looking at the flows into the stream from the spur and hollow areas will show the relative importance of these areas at different times of the year and should help to provide more understanding of water flow pathways within Slapton Wood.

Acknowledgements

The 1989-91 data were collected by the Institute of Hydrology. This monitoring, and the SHETRAN modelling work described here, was funded by UK Nirex Ltd. The author would like to thank John Ewen who designed and wrote SHETRAN Version 5, and also James Bathurst, Tim Burt and an anonymous reviewer, for valuable comments and suggestions.

References

Agata Y, Tanaka Y. 1997. Double-peak storm runoff observed at a hilly watershed in the Soya hills, northern Japan and the conditions in which it occurs with special respect to basin water storage. *Geographical Review of Japan* **70A**: 798-812.

Anderson MG, Burt TP. 1978. The role of topography in controlling throughflow generation. *Earth Surface Processes* **3**: 331-344.

Arnold JG, Srinivasan P, Muttiah RS, Williams JR. 1998. Large area hydrologic modeling and assessment. Part I. Model development. *Journal of the American Water Resources Association* **34**: 73-89.

Bathurst JC, Ewen J, Parkin G, O'Connell PE, Cooper JD. 2004. Validation of catchment models for predicting land-use and climate change impacts. 3. Blind validation for internal and outlet responses. *Journal of Hydrology* **287**: 74-94.

Beven K, Binley A. 1992. The future of distributed models - model calibration and uncertainty prediction. *Hydrological Processes* **6**: 279-298.

Beven K, Freer J. 2001. A dynamic TOPMODEL. *Hydrological Processes* **15**: 1993-2011.

Bingeman AK, Kouwen N, Soulis ED. 2006. Validation of the hydrological processes in a hydrological model. *Journal of Hydraulic Engineering* **11**: 451-463.

Birkinshaw SJ, Ewen J. 2000. Modelling nitrate transport in the Slapton Wood catchment using SHETRAN. *Journal of Hydrology* **230**: 18-33.

Blöschl G, Sivapalan M. 1995. Scale issues in hydrological modelling: a review. *Hydrological Processes* **9**: 251-290.

Borah DK, Bera M. 2003. Watershed-scale hydrologic and nonpoint-source pollution models: Review of mathematical bases. *Transactions of the ASAE* **46**: 1553-1566.

Breuer L, Eckhardt K, Frede H-G. 2003. Plant parameter values for models in temperate climates. *Ecological Modelling* **169**: 237-293.

Burt TP, Arkell BP. 1986. Variable source areas of stream discharge and their relationship to point and non-point sources of nitrate pollution. In *Monitoring to detect changes in water quality series*. IAHS, 157, 155-164.

Burt TP, Butcher DP. 1985a. On the generation of delayed peaks in stream discharge. *Journal of Hydrology* **78**: 361-378.

Burt TP, Butcher DP. 1985b. Topographic controls of soil moisture distributions. *Journal of Soil Science* **36**: 469-486.

Burt TP, Heathwaite AL. 1996. The Hydrology of the Slapton Catchments. *Field Studies* **8**: 543-557.

Burt TP, Horton BP. 2001. The natural history of Slapton Ley National Nature Reserve XXII: the climate of Slapton Ley. *Field Studies* **10**: 35-46.

Butcher DP. 1985. *Field verification of topographic indicies for use in hillslope runoff models*. PhD Thesis, Huddersfield Polytechnic, 491 pp.

Chappell NA, Franks SW. 1996. Property distributions and flow structure in the Slapton Wood catchment. *Field Studies* **8**: 559-575.

Chevallier P, Planchon O. 1993. Hydrological processes in a small humid savanna basin (Ivory- Coast). *Journal of Hydrology* **151**: 173-191.

Coles N, Trudgill ST. 1985. The movement of nitrate fertiliser from the soil surface to drainage waters by preferential flow in weakly structured soils, Slapton, S.Devon. *Agriculture, Ecosystems and Environment* **13**: 241-259.

Ewen J. 2001. *SHETRAN User Manual for Version 5.1, WRSRL/2001_1*, Water Resources Research Laboratory, School of Civil Engineering and Geosciences, University of Newcastle, Newcastle-upon-Tyne, UK.

Ewen J, Birkinshaw SJ. 2006. Lumped hysteretic model for subsurface stormflow developed using downward approach. *Hydrological Processes* **In press**.

Ewen J, O'Donnell G, Burton A, O'Connell E. 2006. Errors and uncertainty in physically-based rainfall-runoff modelling of catchment change effects. *Journal of Hydrology* **330**: 641-650.

Ewen J, Parkin G. 1996. Validation of catchment models for predicting land-use and climate change impacts .1. Method. *Journal of Hydrology* **175**: 583-594.

Ewen J, Parkin G, O'Connell PE. 2000. SHETRAN: Distributed river basin flow and transport modeling system. *Journal of Hydrologic Engineering* **5**: 250-258.

Fisher J. 1995. *The use of remote sensing and other system state estimates in the calibration of a distributed hydrological model*. PhD Thesis, Lancaster University, UK.

Fisher J, Beven KJ. 1996. Modelling of stream flow at Slapton Wood using TOPMODEL within an uncertainty estimation framework. *Field Studies* **8**: 577-584.

Graham DN, Butts MB. 2006. Flexible integrated watershed modelling with MIKE SHE. In *Watershed Models*. V.P. Singh, D.K. Frevert (eds). CRC Press, Boca Raton, 245-272.

Hihara T, Susuki K. 1988. The double peak hydrograph during storm events in a small watershed of the Tama hills, west of Tokyo. *Geographical Review of Japan* **61A**: 804-815.

Hirose T, Onda Y, Matsukura Y. 1994. Runoff characteristics and solute concentration on four small catchments with different bedrocks in the Abukuma mountains Japan. *Transactions Japanese Geomorphological Union* **15A**: 31-48.

Institute of Hydrology. 1993. *The Slapton Ley NERC airborne campaign - the results of image analysis and their relevance to the hydrology of the catchment*, Wallingford, Oxford, UK.

Lakey B, Krothe NC. 1996. Stable isotopic variation of storm discharge from a perennial karst spring, Indiana. *Water Resources Research* **32**: 721-731.

Onda Y, Komatsu Y, Tsujimura M, Fujihara J. 2001. The role of subsurface runoff through bedrock on storm flow generation. *Hydrological Processes* **15**: 1693-1706.

Panday S, Huyakorn PS. 2004. A fully coupled physically-based spatially-distributed model for evaluating surface/subsurface flow. *Advances in Water Resources* **27**: 361-382.

Panday S, Huyakorn PS, Therrien R, Nichols RL. 1993. Improved three-dimensional finite-element techniques for field simulation of variably saturated flow and transport. *Journal of Contaminant Hydrology* **12**: 3-33.

Trudgill ST. 1983. The natural history of Slapton Ley Nature Reserve, XVI: the soils of Slapton Wood. *Field Studies* **5**: 833-840.

Weyman DR. 1973. Measurements of the downslope flow of water in a soil. *Journal of Hydrology* **20**: 267-288.

Zhang XX, Ewen J. 2000. Efficient method for simulating gravity-dominated water flow in unsaturated soils. *Water Resources Research* **36**: 2777-2780.

Table I. Main parameter values for 1D Simulations. (*calibrated)

Parameter	Arable	Grassland	Woodland
Bottom boundary volumetric percolation flux (2m below ground)	2.3×10^{-8} m/s*	2.1×10^{-8} m/s*	2.0×10^{-8} m/s*
Bottom boundary temperature (2m below ground)	10ºC	10ºC	10ºC
Transpiration reduction factor at –3.3m head	0.4*	0.4*	0.28*
Canopy storage capacity	5×10^{-4} m	1×10^{-4} m	15×10^{-4} m
Canopy resistance	80 s/m	100 s/m	150 s/m
Maximum vegetation height	0.7m	0.3m	5.0m
Maximum fraction of energy absorbed by the canopy	0.8	0.9	0.8
Maximum rooting depth	0.5 m	0.3 m	2.0 m
Maximum leaf area index	1.0	1.6	4.0

Table II. Annual evaporation, for 1-D simulations (mm)

Plot	Simulated canopy evaporation	Simulated surface evaporation	Simulated transpiration	Totals simulated	Total estimated from measurement
Arable	43	14	332	389	404
Grassland	96	12	354	461	466
Woodland	201	19	298	518	487

Table III. Main parameter values for 2-D simulations (* calibrated)

Soil	Saturated moisture content (-)	Residual moisture content (-)	Saturated hydraulic conductivity (m/day)	Van Genuchten α parameter (/m)	Van Genuchten n parameter (-)
Clay loam 1 (0 - 1.5m below ground)	0.4	0.12	0.5	1.0	1.6
Clay loam 2 (1.5m – 2.2m below ground)	0.4	0.12	300.0*	100.0*	1.1*
Slate 1 (2.2m – 2.7m below ground)	0.18	0.03	0.01*	2.68	1.92
Slate 2 (2.7m – 20.0m below ground)	0.18	0.03	0.1*	2.68	1.92
Clay loam under stream (0 - 2.2m below stream)	0.4	0.12	7.0*	1.0	1.6

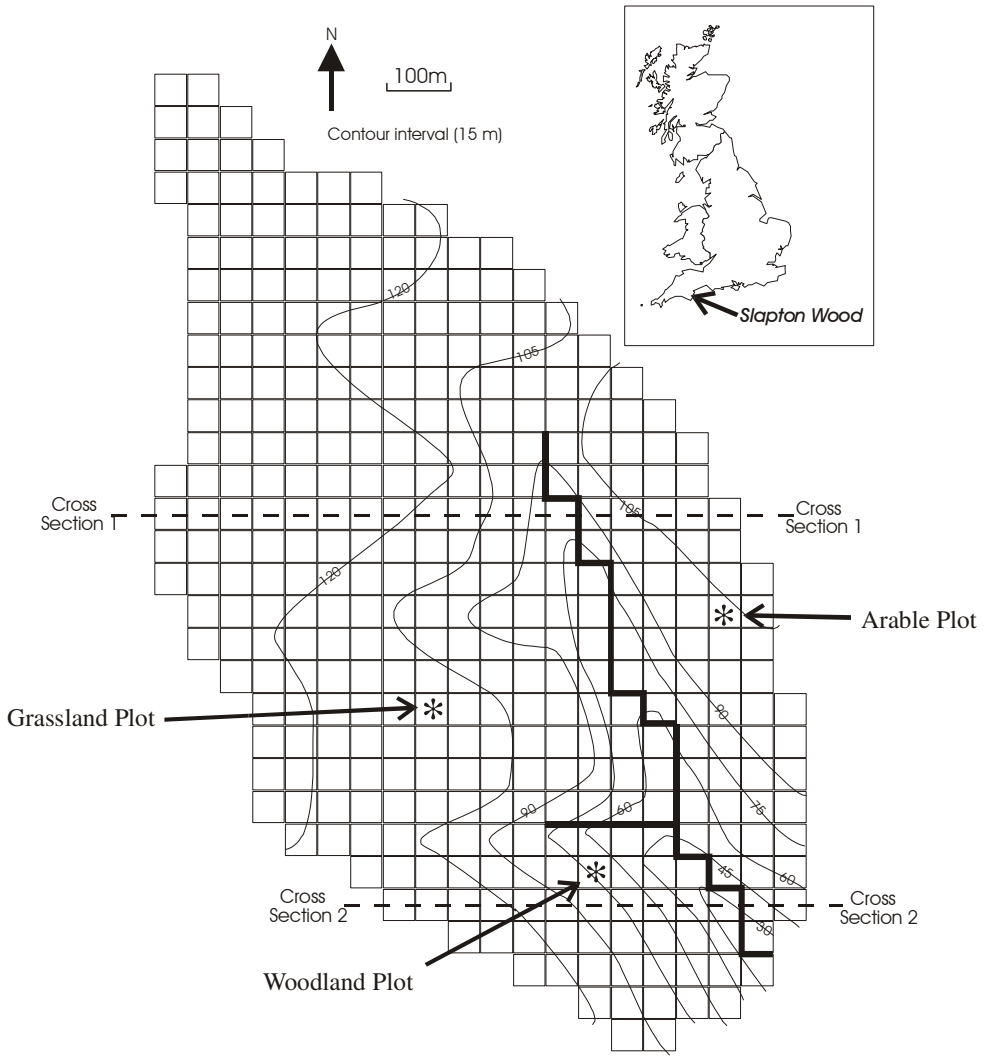

Figure 1. Location map and SHETRAN mesh for the Slapton Wood catchment. The SHETRAN mesh shows the channel network in bold

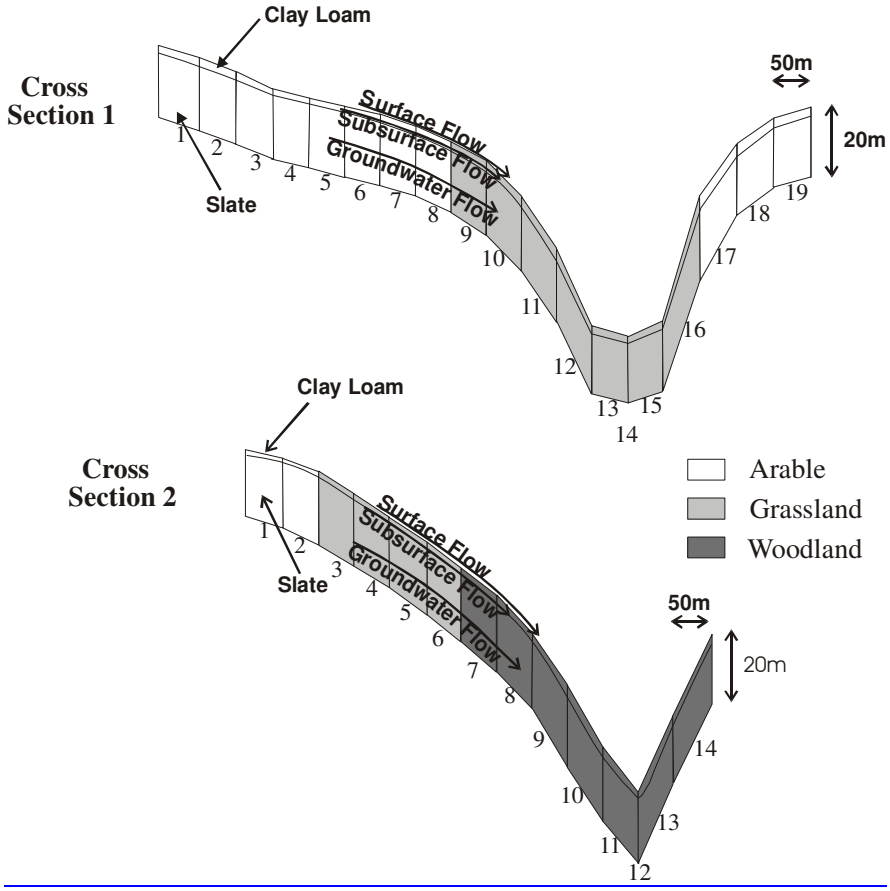

Figure 2. Slapton Wood cross-sections and sub-units (numbered)

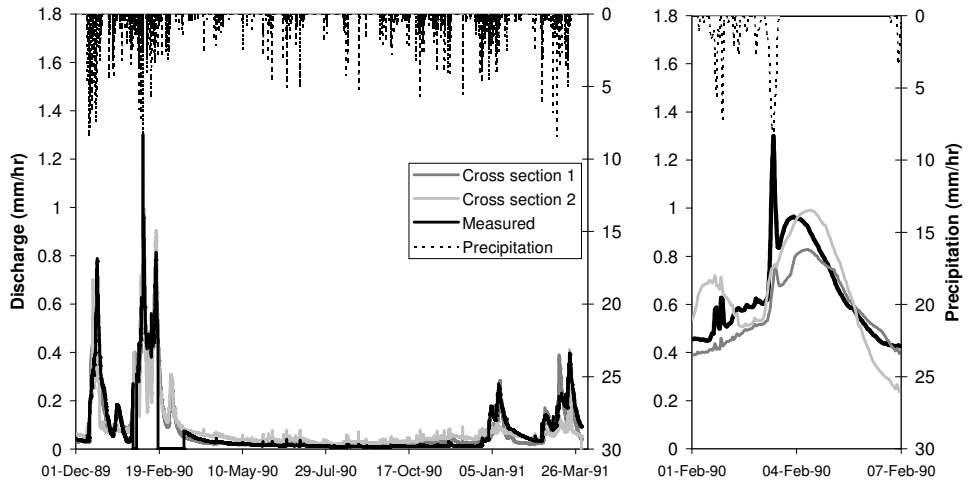

Figure 3. Measured discharge at the catchment outlet and simulated discharge from the two cross-sections (the measurement flume was blocked by sediment from 15th February 1990 to 10th March 1990)

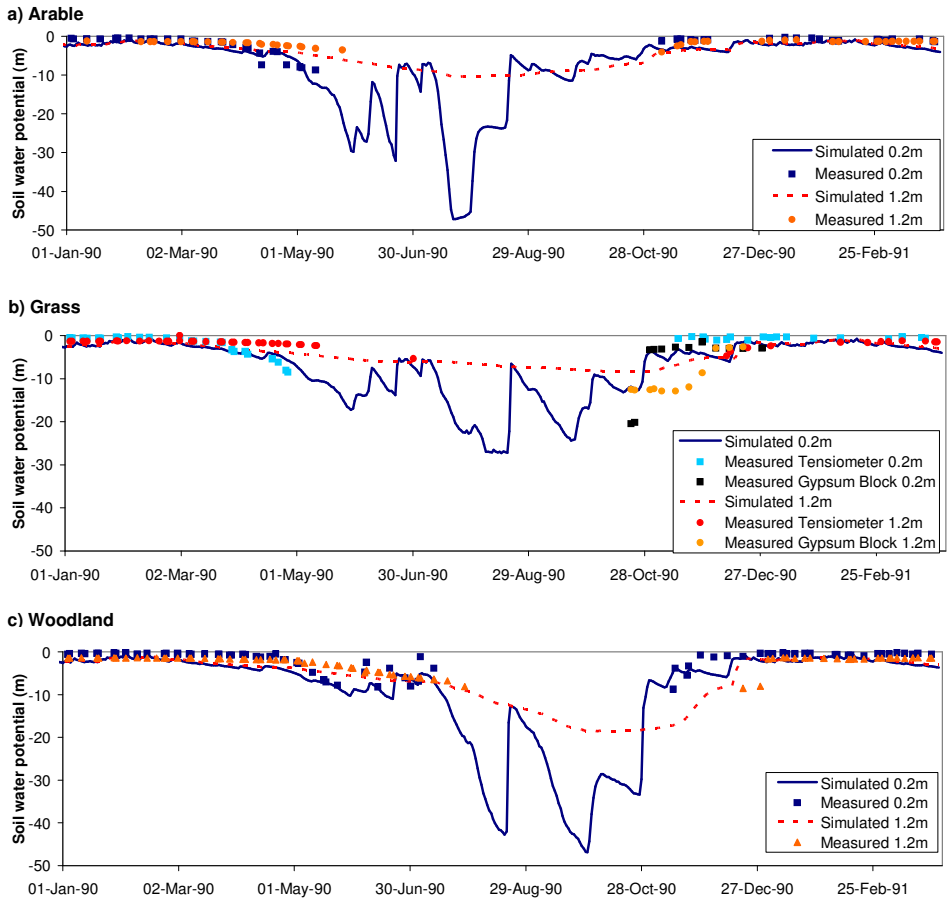

Figure 4. Simulated and measured soil water potentials

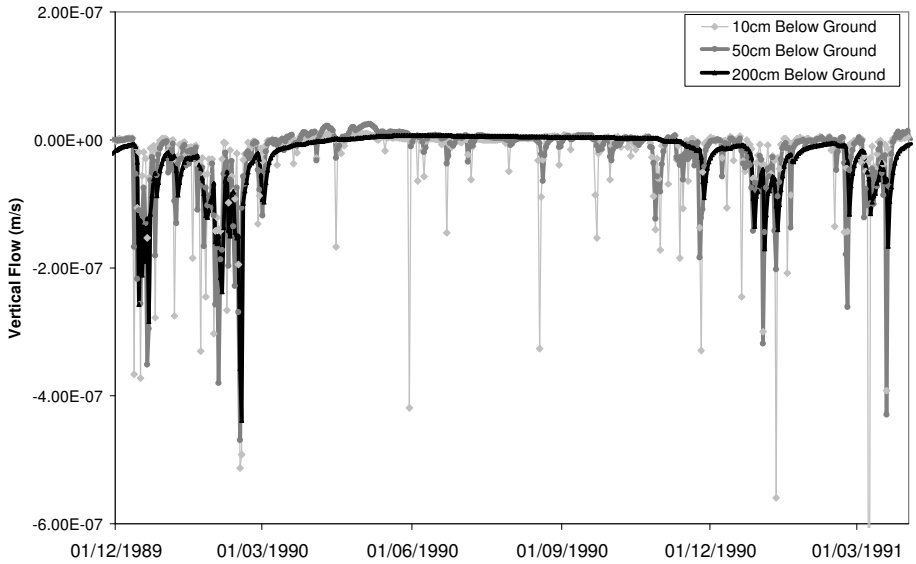

Figure 5. Vertical flows at three depths in sub-unit 4 cross-section 1

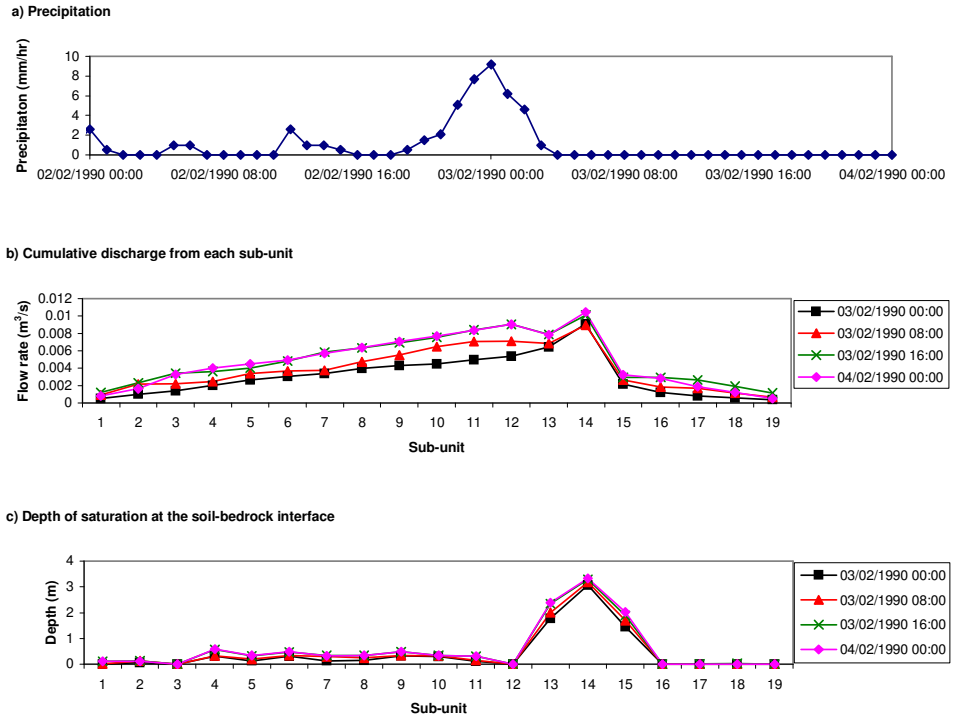

Figure 6. Delayed response for cross-section 1 for an event on 3rd February 1990. Sub-unit 14 is the river channel.

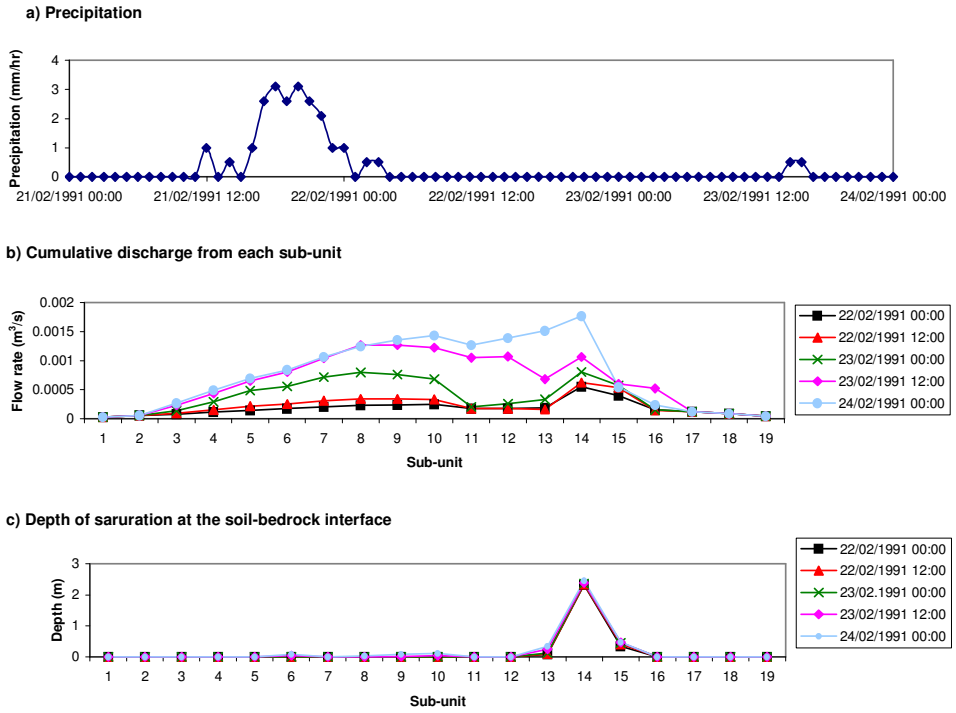

Figure 7. Delayed response for cross-section 1 for an event on 22nd February 1991. Sub-unit 14 is the river channel.

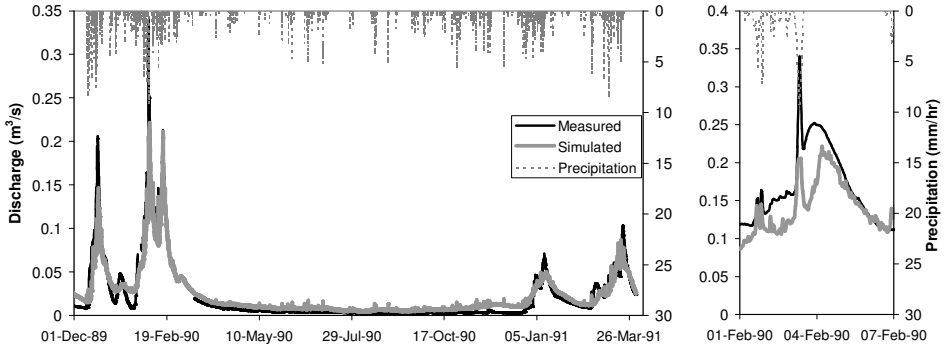

Figure 8. Measured and simulated discharge at the catchment outlet (the measurement flume was blocked by sediment from 15th February 1990 to 10th March 1990)

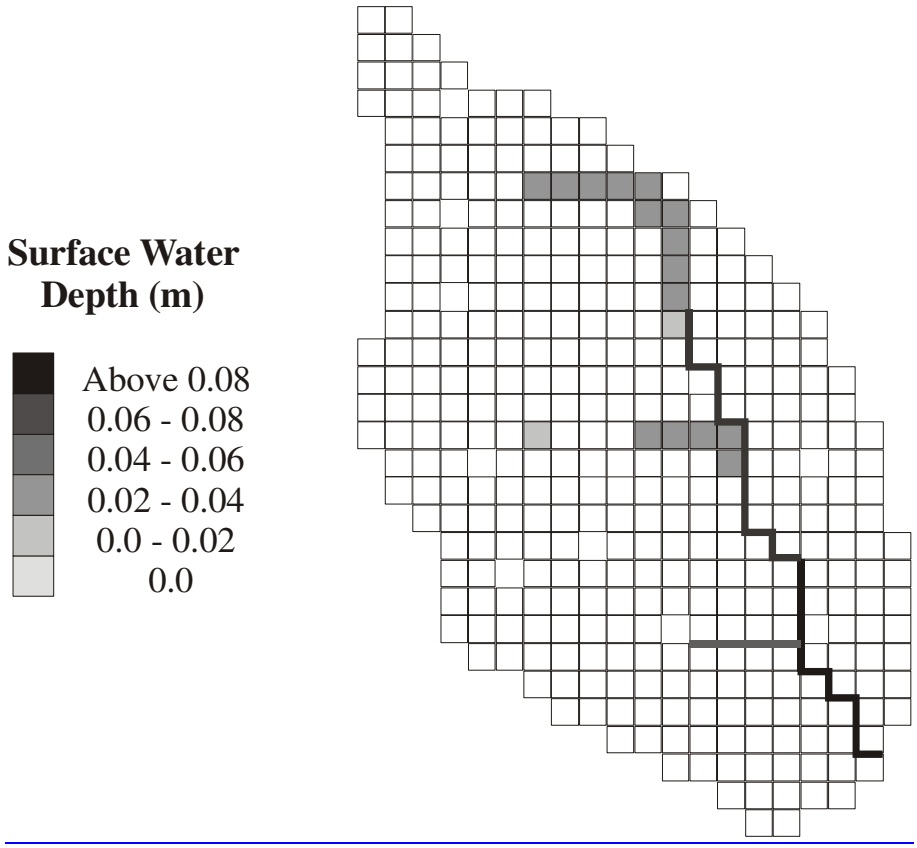

Figure 9. Simulated surface water depth on 3rd February 1990

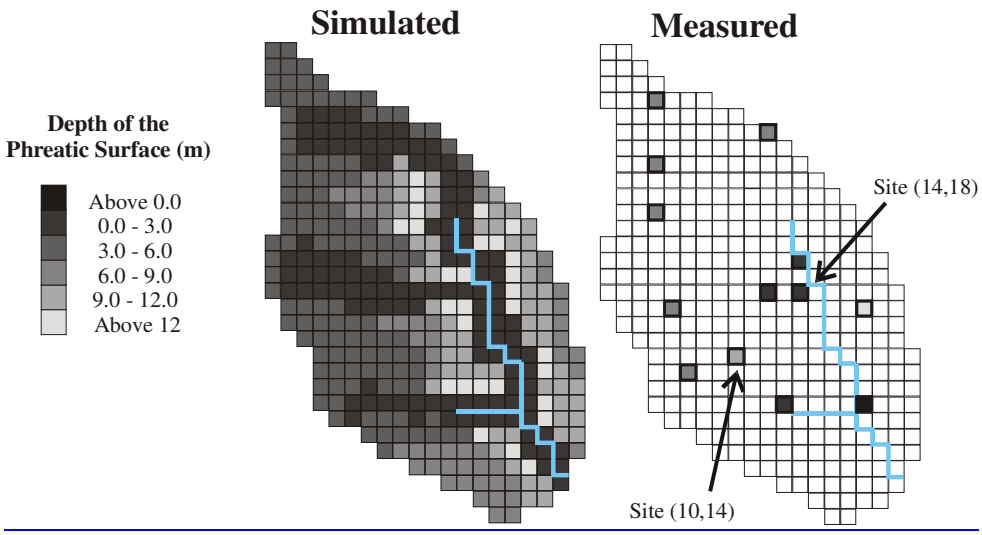

Figure 10. Simulated and measured phreatic surface levels on 10th October 1990

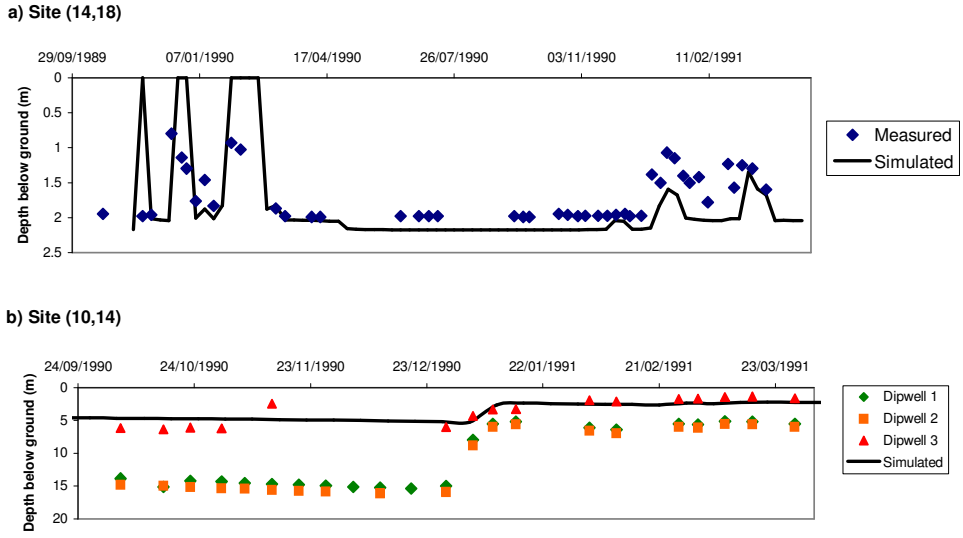

Figure 11. Simulated and measured phreatic surface levels at two sites